

NMR Assignment of des [40-93] Mutant of Bovine Angiogenin

Woonghee Kim,[†] Sun-Hee Back,[†] Dong-II Kang,[‡] Hang-Cheol Shin,[§] and Yangmee Kim^{†,*}

[†]Department of Bioscience and Biotechnology, Konkuk University, Seoul 143-701, Korea. *E-mail: ymkim@konkuk.ac.kr

[‡]Department of Chemistry, Konkuk University, Seoul 143-701, Korea

[§]Department of Bioinformatics and Life Science, and CAMDRS, Soongsil University, Seoul 156-743, Korea

Received September 17, 2008

Angiogenin is a potent inducer of blood vessel formation and is overexpressed in many cancers. It is a member of the pancreatic RNase superfamily. Angiogenin has 33% sequence identity with RNase A. All RNases family proteins except angiogenin and turtle RNase have four disulfide bonds. Angiogenin has three disulfide bonds, [C27-C82], [C40-C93] and [C58-C108], respectively. To examine the role of disulfide bond [C40-C93] near the nuclear localization site, recombinant des [40-93] mutant by replacement of cysteines at positions 40 and 93 with serines was cloned, expressed, and purified. CD spectrum of des [40-93] was similar to that of wild type and implies that the overall folding of two forms is similar. 2D and 3D NMR experiments for ¹⁵N and/or ¹³C-isotope labeled des [40-93] were performed and the backbone resonance assignment was done. Based on the result of backbone assignment and chemical shift index (CSI), we confirmed that deletion of [C40-C93] disulfide bond affected the local structural stability of bovine angiogenin near the nuclear localization site and ribonucleolytic active site. Based on this assignment, studies on structure and dynamics of des [40-93] mutant will be performed.

Key Words : Angiogenin, des [40-93], NMR, Assignment, Angiogenesis

Introduction

Angiogenesis is a complex process to form new blood vessel, which is essential for cell reproduction, development and wound repair under normal condition. This process involves endothelial cell proliferation, migration and membrane degradation. A variety of pathological conditions are also importantly dependent on angiogenesis. Since angiogenesis is important for the growth and metastasis of tumors, many studies are being focused on the understanding of angiogenesis. Therefore, its inhibitors have received particular attention because of their therapeutic potential.^{1,2} The formation of new blood vessels is crucial for tissue regeneration and for efficient tumor growth, and requires the concerted action of various angiogenic factors and inhibitors.³

Angiogenin is one of the angiogenic factors and is related to tumor growth and metastasis.⁴ Inhibition of the growth, progression, and metastasis of tumor has been shown using several antiangiogenic modalities. These inhibitory techniques include blocking antibodies specific to angiogenin, antisense oligonucleotide blockade of angiogenin, and small molecule inhibitors of other angiogenic peptides. Specifically, angiogenin antagonists have been shown to inhibit tumor growth.^{4,5} Angiogenin is a member of the pancreatic ribonuclease (RNase A) superfamily and the primary structure of angiogenin is highly homologous to that of the pancreatic ribonucleases.^{6,7} Bovine Angiogenin (bAng) consists of 125 amino acids and has about 33% sequence identity with RNase A. The three dimensional structures of bAng and human angiogenin (hAng) have been determined by X-ray crystallography and nuclear magnetic resonance spectro-

scopy.⁸⁻¹² ¹H Resonance assignment of wild type bAng (WT bAng) has been done by Spik group based on COSY and NOESY spectra.¹³

Although overall folding of angiogenin is similar to that of RNase A, angiogenin contains unique functional features that account for its angiogenesis while RNase A does not

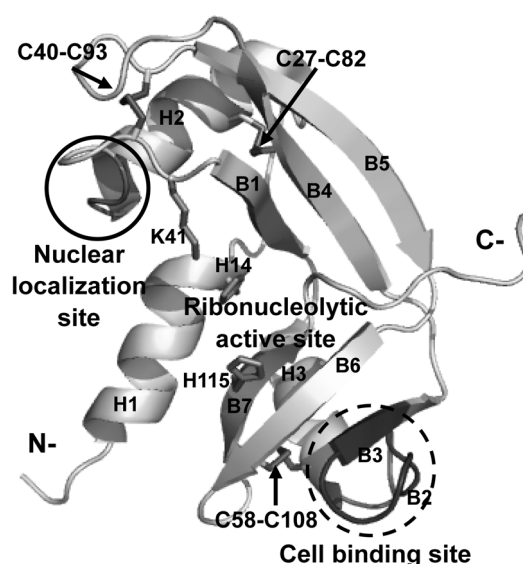


Figure 1. A representation of 3D structure of WT bAng. This protein has three α -helices and seven β -sheets. The C40-C93 disulfide bond is located in a vicinity of nuclear localization site (solid circle). Dashed circle represent the cell binding site. H14, K41, H115 are the three important residues at ribonucleolytic active site. Three arrows point at disulfide bonds, [C27-C82], [C40-C93], and [C58-C108]. The figure was prepared with PyMol⁴¹ with the PDB coordinate file 1AGI.¹²

have angiogenic activity.¹⁴ Angiogenin was first isolated from the conditioned medium of a human adenocarcinoma¹⁵ and was identified as a component of normal human plasma.¹⁶ Nuclear angiogenin assumes an essential role in endothelial cell proliferation and is necessary for angiogenesis induced by other angiogenic factors.¹⁷ Exhaustive preceding studies of structure and function relationships have demonstrated that three sites, a ribonucleolytic active site,¹⁸ an endothelial cell binding site¹⁹ and a nuclear localization site²⁰ are essential for angiogenic activity.²¹ As shown in Figure 1, the ribonucleolytic active site is a cleft including H14, K41, and H115 residues at the junction of helix H1, strands B1 and B7.²² The endothelial cell binding site is located between strands B2 and B3. The nuclear localization site is located at an exposed loop region between helix H2 and strand B1. Most proteins in RNase A superfamily except for angiogenin and turtle RNase have four disulfide bonds. The three disulfide bonds of angiogenin, [C27-C82], [C40-C93], and [C58-C108], respectively, provide the stability of the spatial structure of this protein.²²⁻²⁵

In this study, to investigate the role of disulfide bonds, recombinant des [40-93] mutant by replacement of C40 and C93 with S40 and S93 was cloned, expressed, and purified. CD and 2D, 3D NMR experiments were performed to observe the structural difference between the WT bAng and the des [40-93] mutant. This result will provide the important insight to the further structural studies of angiogenin and development of the anticancer drug.

Methods

Expression and purification of WT bAng and des [40-93]. The recombinant WT bAng and des [40-93] were previously cloned into a pET-21a(+) (Novagen) vector containing an IPTG inducible promoter and resistance to ampicillin.²⁶ This vector was transformed into the *E. coli* strain Rosetta (DE3) pLysS for expression of bovine angiogenin. Angiogenin was expressed in an insoluble form. The insoluble pellet obtained after complete sonication of cells was dissolved in 0.1 M Tris-HCl buffer (pH 8.0) containing 6 M Gu-HCl, 1 mM EDTA, 0.1 M NaCl and 10 mM reduced dithiothreitol (DTT^{red}). The soluble extract was then slowly diluted for refolding with 0.1 M Tris-HCl (pH 8.0), 1 mM EDTA, 0.3 mM oxidized glutathione (GSSG), 1.5 mM reduced glutathione (GSH) and then incubated for 2 weeks

at 277 K. The same amount of 25 mM Tris-HCl buffer (pH 8.0) was mixed with refolding buffer. Refolding buffer of bAng des [40-93] was concentrated to 30 mL, after mixing with 100 mM AcOH. The refolded protein was purified using a cation-exchange FPLC column and equilibrated with 25 mM Tris-HCl buffer (pH 8.0), eluted with 1 M NaCl gradient. Further purification was carried out by gel filtration chromatography and equilibrated with 50 mM sodium phosphate buffer (pH 7.0), 150 mM NaCl. The WT bAng fractions collected from the gel filtration chromatography were dialyzed against water for 24 h at 277 K. The des [40-93] was dialyzed against 100 mM acetic acid and the protein sample was lyophilized. ¹³C/¹⁵N or ¹⁵N-isotopically labeled protein samples were prepared by growing cells in the M9 minimal media containing ¹⁵NH₄Cl (Cambridge Isotope Laboratories), either with or without ¹³C₆-D-glucose (Cambridge Isotope Laboratories) as the sole source of nitrogen and carbon.

Circular dichroism. Circular Dichroism (CD) experiments were performed by using a J-810 (JASCO, Tokyo, Japan) spectropolarimeter with 1-mm path length cell. To investigate the difference of the secondary structure of both type proteins, we recorded the far UV CD spectra in 0.1 nm intervals from 190 to 250 nm at 298 K. Protein samples were prepared in 50 mM sodium phosphate buffer, 150 mM NaCl at pH 5.5. For each spectrum, the data from 10 scans was averaged and smoothed using J-810.

NMR spectroscopy. All NMR experiments were performed on 1.0 mM with ¹³C/¹⁵N-labeled and ¹⁵N-labeled WT bAng and des [40-93]. All NMR spectra were recorded on a Bruker Avance-800 MHz spectrometer at Korea Basic Science Institute. The acquisition parameters for these experiments are listed in Table 1. The backbone assignment was started by picking cross-peaks in a two-dimensional ¹H-¹⁵N HSQC, to obtain HN(i) and ¹⁵N(i) resonance frequencies. The backbone assignments were accomplished using the HNCA, HNCACB and CBCA(CO)NH spectra. The sequential assignment by triple resonance data were confirmed by 3D ¹H-¹⁵N TOCSY-HSQC spectrum with a 60 ms isotropic mixing time and 3D ¹H-¹⁵N NOESY-HSQC spectrum with a 150 ms mixing time as identifying d_{NN(i, i+1)} and d_{αN(i, i+1)} sequential NOEs. Three-dimension triple-resonance experiments were performed on a ¹³C/¹⁵N-labeled uniformly double labeled sample in 50 mM sodium phosphate buffer, 150 mM NaCl at pH 5.5.²⁹⁻³⁵ Proton chemical shifts were

Table 1. Acquisition parameters for experiments

Experiment	Nucleus			No. of complex points			SW (ppm)			Scans
	F1	F2	F3	F1	F2	F3	F1	F2	F3	
HNCA	¹⁵ N	¹³ C ^α	¹ H ^N	48	128	2048	50	40	5.5	8
CBCA(CO)NH	¹⁵ N	¹³ C ^{α/β}	¹ H ^N	48	128	2048	50	80	4	8
HNCACB	¹⁵ N	¹³ C ^{α/β}	¹ H ^N	48	128	2048	50	80	4	8
TOCSY-HSQC	¹ H	¹⁵ N	¹ H ^N	128	48	2048	11	50	5.5	16
NOESY-HSQC	¹ H	¹⁵ N	¹ H ^N	128	48	2048	11	50	5.5	16
HSQC	¹⁵ N	¹ H ^N					50	4		2

referenced to DSS (2,2-dimethyl-2-silapentane-5-sulfonate) at 0 ppm.²⁷ All spectra were recorded at 298 K and NMR data was processed with the programs nmrPipe²⁸ and visualized with Sparky.²⁹

Results and Discussion

According to the crystallographic studies and site-directed mutagenesis on hAng, T44 and residues 38-41 near the disulfide bond [C39-C92] of human angiogenin play important roles on the enzyme activity and pyrimidine specificity.³⁰ The residues from R31 to R33 in hAng are known to be involved in nuclear translocation near the disulfide bond [C39-C92], too.³¹ Therefore, the deletion of [40-93] disulfide bond in bAng by substitution of C40 and C93 with S40 and S93 may also affect its biological activity as well as its structure. Therefore, in this study, des [40-93] mutant was expressed and purified with over 95% purity. Also, CD experiments and the NMR assignments of des [40-93] were performed.

CD spectra of WT bAng and des [40-93] at 298 K are shown in Figure 2. Even though des [40-93] does not have a [C40-C93] disulfide bond, both types have very similar contents of α -helical and β -sheet structures. CD results imply that two proteins have similar overall structures.

¹³C/¹⁵N or ¹⁵N-labeled bAng des [40-93] was expressed and purified. The strip plots of ¹³C α and ¹³C β carbons of HNCACB (A) and HNCA (B) spectra from K55 to N62 of des [40-93] are shown in Figure 3. The sequence-specific resonance assignment was carried out by using standard procedures and mainly using CBCA(CO)NH and HNCACB.³²⁻³⁸ The sequential assignments were confirmed by 3D ¹H-¹⁵N TOCSY-HSQC and ¹H-¹⁵N NOESY-HSQC spectra.

A total of 91 out of 118 non-proline residues of HSQC spectrum of bAng des [40-93] could be assigned. Residues L11, N52, D53, and I72 were not able to be assigned because of the spectral overlapping. Peaks of HNCACB and NOESY-HSQC of residues such as K32, T37, residues from P39 to F46, and residues from K83 to K85, residues from

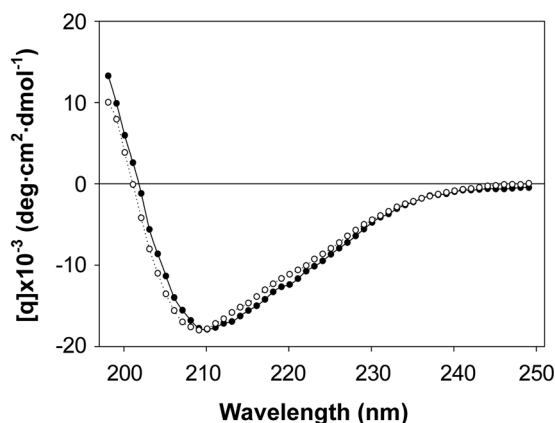


Figure 2. CD spectra of WT bAng and des [40-93] in 50 mM sodium phosphate buffer, 150 mM NaCl (pH 5.5). Spectrum of WT bAng is depicted with filled circle and that of bAng des [40-93] is depicted with open circle.

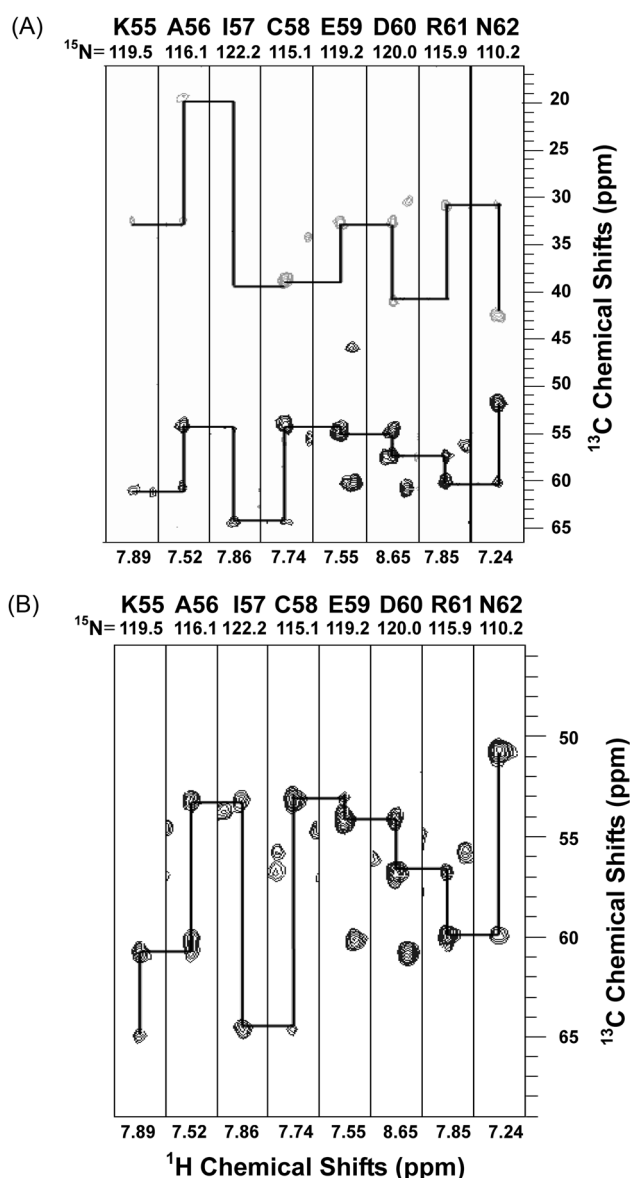


Figure 3. Strip plot of data extracted from HNCACB, HNCA spectra of bAng des [40-93]. (A) Strip plot of HNCACB spectra. Resonances of ¹³C β are depicted in bright gray and the resonances of ¹³C α are depicted in black. (B) Strip plot of HNCA spectra. ¹H/¹³C slices from 3D triple-resonance experiments representing sequential backbone resonance assignment for residues from K55 to N62.

P91 to R94 in the vicinity of S40 and S93, which were substituted for C40 and C93 in bAng, were not appeared because of structural flexibility. The chemical shift values of the ¹HN, ¹⁵N, ¹³C α and ¹³C β resonances of des [40-93] are listed in Supplementary material.

HSQC spectrum was well resolved and chemical shift dispersions were suitable for resonance assignments. The superimposed two-dimensional ¹H-¹⁵N HSQC spectra of WT bAng and des [40-93] are shown in Figure 4. Chemical shift deviations in HSQC spectra between WT bAng and des [40-93] are depicted with bar graph in Figure 5(A). Deletion of disulfide bond [40-93] resulted in disappearance of the

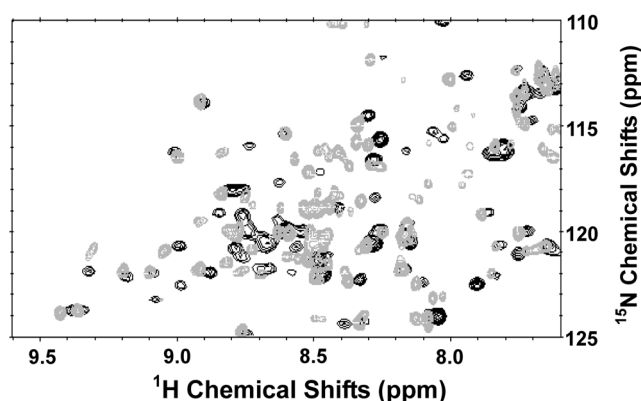


Figure 4. Overlay of two-dimensional ^1H - ^{15}N HSQC spectra of the WT bAng (black) and des [40-93] (bright gray) forms.

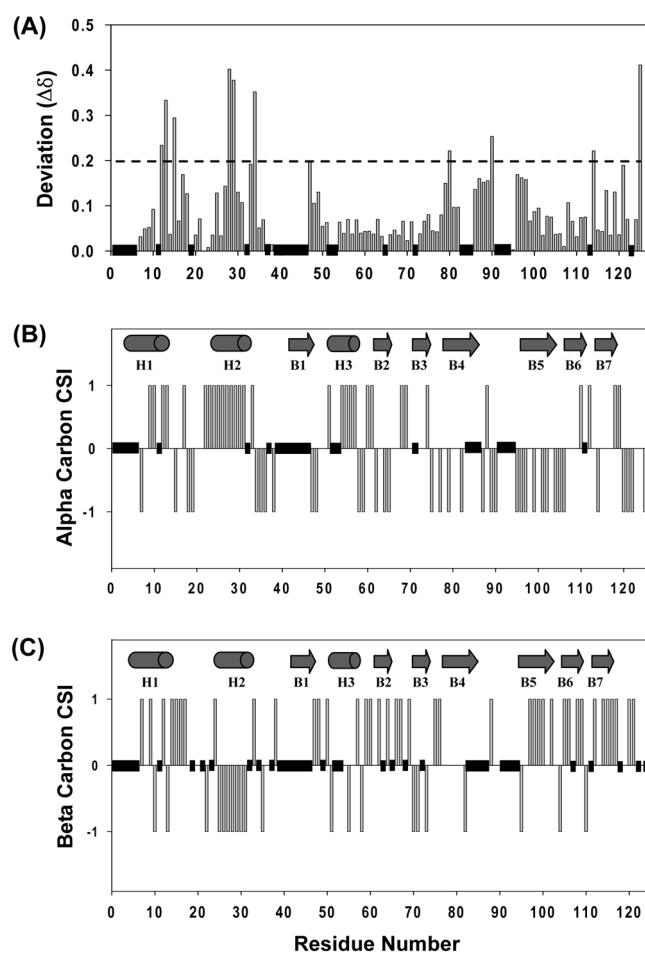


Figure 5. (A) Chemical shift changes in bAng induced by elimination of [40-93] disulfide bond. $\Delta\delta_{\text{av}} = \{0.5[\Delta\delta(^1\text{H}^{\text{N}})^2 + (0.2\Delta\delta(^{15}\text{N}))^2]\}^{1/2}$ where $\Delta\delta(^1\text{H}^{\text{N}})$ and $\Delta\delta(^{15}\text{N})$ are the chemical shift differences for the $^1\text{H}^{\text{N}}$ and ^{15}N atoms⁴² between wild type and des [40-93]. Black rectangles in graph represent the prolines and the residues which are not appeared in the spectra because of the structural flexibility. Backbone ^{13}C consensus CSI plots of bAng des [40-93] based on resonance assignments. (B) Chemical Shift Index derived from $^{13}\text{C}^\alpha$ chemical shifts, (C) Chemical Shift Index derived from $^{13}\text{C}^\beta$ chemical shifts. Gray cylinders represent the α -helix region and gray arrows represent the β -sheet region based on the X-ray structure of WT bAng.¹²

resonances from many residues near S40 and S93 because of the structural flexibility and some of them showed large deviations compared to those in the other regions. There were large deviations near H1, H2, B4 and the loop region connecting B4 and B5. We also utilized consensus CSI, which is regarded as the best method to provide information about the secondary structures, based on the chemical shift values of C^α and C^β .³⁸⁻⁴⁰ CSI of des [40-93] on the basis of resonance assignments are shown in Figure 5(B) and (C). Positive C^α and negative C^β indicate that the residue commonly assumes an α -helix, whereas the opposite signs indicate a β -sheet structure. CSI of des [40-93] for the C^α chemical shifts of some residues in strand B3 and B7 were not negative as shown in Figure 5(B), CSI for the C^β chemical shifts of residues at H1, B3, and B4 also show deviations from the secondary structure of the WT bAng as shown in Figure 5(C). From the resonance disappearance and assignments, it can be assumed that helix H1, H2 of des [40-93] at the N-terminus are more flexible than those of WT bAng. Also, it can be assumed that the elimination of [C40-C93] disulfide bond may affect the stability of ribonucleolytic site as well as nuclear localization site including these motives. It can affect the structural stability and dynamics of bAng, too.

Even though CD spectra implied that overall folding of two forms are very similar, dynamics of two forms should be very different. We will investigate the biological activities and the dynamics of des [40-93] compared to WT bAng based on these resonance assignments. Furthermore, lead compound of bAng inhibitor will be screened by *in silico* screening and NMR spectroscopy using WT bAng and des [40-93]. This study will be helpful to develop new inhibitors of bAng as potent cancer drug.

Acknowledgments. This work was supported by the Research Program for New Drug Target Discovery (M10601000153-07N0100-15310) grant from the Ministry of Science & Technology, South Korea and the Soongsil University Research Fund. This work was partly supported by a grant (20080401-034-017) from Biogreen 21 program, Rural Development Administration, Republic of Korea. Woonghee Kim is supported, in part, by the second BK21 (MOE).

Supporting Information. The list of the chemical shift values of the ^1HN , ^{15}N , $^{13}\text{C}^\alpha$ and $^{13}\text{C}^\beta$ resonances of des [40-93] is available at <http://www.kcsnet.or.kr/bkcs> or on request from the correspondence author.

References

- Folkman, J.; Klagsbrun, M. *Science* **1987**, *235*, 442.
- Folkman, J.; Cotran, R. S. *Int. Rev. Exp. Path.* **1976**, *16*, 207.
- Folkman, J. *Nat. Med.* **1995**, *1*, 27.
- Katona, T. M.; Neubauer, B. L.; Iversen, P. W.; Zhang, S.; Baldrige, L. A.; Cheng, L. *Clin Cancer Res.* **2005**, *11*, 8358.
- Stoeltzing, O.; Liu, W.; Reinmuth, N.; Parikh, A.; Ahmad, S. A.;

- Jung, Y. D.; Fan, F.; Ellis, L. M. *Annals of Surgical Oncology* **2002**, *10*, 722.
6. Strydom, D. J.; Fett, J. W.; Lobb, R. R.; Alderman, E. M.; Bethune, J. L.; Riordan, J. F.; Vallee, B. L. *Biochemistry* **1985**, *24*, 5486.
7. Kurachi, K.; Davie, E. W.; Strydom, D. J.; Riordan, J. F.; Vallee, B. L. *Biochemistry* **1985**, *24*, 5494.
8. Acharya, K. R.; Shapiro, R.; Allen, S. C.; Riordan, J. F.; Vallee, B. L. *Proc. Natl. Acad. Sci. U.S.A.* **1994**, *91*, 2915.
9. Chrisine, R.; Daniel, A.; Francois, B.; Jean-Yves, L.; Jean-Pierre, D.; Genevieve, S. *Eur. J. Biochem.* **1994**, *224*, 811.
10. Lequin, O.; Albaret, C.; Bontems, F.; Spik, G.; Lallemand, J. Y. *Biochemistry* **1996**, *35*, 8870.
11. Lequin, O.; Thuring, H.; Robin, M.; Lallemand, J. Y. *Eur. J. Biochem.* **1997**, *250*, 712.
12. Acharya, K. R.; Shapiro, R.; Riordan, J. F.; Vallee, B. L. *Proc. Natl. Acad. Sci. U.S.A.* **1995**, *92*, 2949.
13. Reisdorf, C.; Abergel, D.; Bontems, F.; Lallemand, J.-Y.; Decottignies, J.-P.; Spik, G. *Eur. J. Biochem.* **1994**, *224*, 811.
14. Shapiro, R.; Riordan, J. F.; Vallee, B. L. *Biochemistry* **1986**, *25*, 3527.
15. Fett, J. W.; Strydom, D. J.; Lobb, R. R.; Alderman, E. M.; Bethune, J. L.; Riordan, J. F.; Vallee, B. L. *Biochemistry* **1985**, *24*, 5480.
16. Shapiro, R.; Strydom, D. J.; Olson, K. A.; Vallee, B. L. *Biochemistry* **1987**, *26*, 5141.
17. Kishimoto, K.; Liu, S.; Tsuji, T.; Olson, K. A.; Hu, G. F. *Oncogene* **2005**, *24*, 445.
18. Shapiro, R.; Vallee, B. L. *Biochemistry* **1989**, *28*, 7401.
19. Hallahan, T. W.; Shapiro, R.; Strydom, D. J.; Vallee, B. L. *Biochemistry* **1992**, *31*, 8022.
20. Moroianu, J.; Riordan, J. F. *Proc. Natl. Acad. Sci. U.S.A.* **1994**, *91*, 1677.
21. Hallahan, T. W.; Shapiro, R.; Vallee, B. L. *Proc. Natl. Acad. Sci. U.S.A.* **1991**, *88*, 2222.
22. Lequin, O.; Albaret, C.; Bontems, F.; Spik, G.; Lallemand, J. Y. *Biochemistry* **1996**, *35*, 8870.
23. Vallee, B. L.; Riordan, J. F. *Cell. Mol. Life Sci.* **1997**, *53*, 803.
24. Smith, B. D.; Raines, R. T. *Protein Engineering, Design & Selection* **2007**, *1*.
25. Zhang, J. *Mol. Biol. Evol.* **2007**, *24*, 505.
26. Jang, S. H.; Kang, D. K.; Chang, S. I.; Scheraga, H. A.; Shin, H. C. *Biotechnol. Lett.* **2004**, *26*, 1501.
27. Wishart, D. S.; Sykes, B. D. *Methods Enzymol.* **1994**, *239*, 363.
28. Delaglio, F.; Grzesiak, S.; Vuister, W. G.; Zhu, G.; Pfeifer, J.; Bax, A. *J. Biomol. NMR* **1995**, *6*, 277.
29. Goddard, T. D.; Kneller, D. G. *SPARKY 3*; University of California: San Francisco, 2003.
30. Holloway, D. E.; Chavali, G. B.; Hares, M. C.; Baker, M. D.; Subbarao, G. V.; Shapiro, R.; Acharya, K. R. *Biochemistry* **2004**, *43*, 1230.
31. Moroianu, J.; Riordan, J. F. *Proc. Natl. Acad. Sci. U.S.A.* **1994**, *91*, 1677.
32. Wuthrich, K. *NMR of Proteins and Nucleic Acids*; John Wiley & Sons: 1986; pp 176-199.
33. Gronenborn, A. M.; Bax, A.; Wingfield, P. T.; Clore, M. *FEBS Lett.* **1989**, *243*, 93.
34. Kang, D. I.; Jung, K. W.; Kim, S.; Lee, S.-A.; Jhon, G.-J.; Kim, Y. *Bull. Korean Chem. Soc.* **2007**, *28*, 2209.
35. Chae, Y. K.; Lee, H.; Lee, W. *Bull. Korean Chem. Soc.* **2007**, *28*, 1549.
36. Grzesiek, S.; Bax, A. *J. Biomol. NMR* **1993**, *3*, 185.
37. Wittekind, M.; Mueller, L. *J. Mag. Res. Series B* **1993**, *101*, 201.
38. Meissner, A.; Sorensen, O. W. *J. Mag. Res. Series B* **2001**, *151*, 328.
39. Wishart, D. S.; Sykes, B. D. *J. Biomol. NMR* **1994**, *4*, 171.
40. Wishart, D. S.; Sykes, B. D.; Richards, F. M. *Biochemistry* **1992**, *31*, 1647.
-